AIP | Applied Physics Letters

Surface polar states and pyroelectricity in ferroelastics induced by flexo-roto field

A. N. Morozovska, E. A. Eliseev, S. V. Kalinin, Long Qing Chen, and Venkatraman Gopalan

Citation: Appl. Phys. Lett. **100**, 142902 (2012); doi: 10.1063/1.3701152
View online: http://dx.doi.org/10.1063/1.3701152
View Table of Contents: http://apl.aip.org/resource/1/APPLAB/v100/i14
Published by the American Institute of Physics.

Surface polar states and pyroelectricity in ferroelastics induced by flexo-roto field

A. N. Morozovska,[1,2] E. A. Eliseev,[2] S. V. Kalinin,[3] Long Qing Chen,[4] and Venkatraman Gopalan[4]
[1]*Institute of Semiconductor Physics, National Academy of Science of Ukraine, 41, pr. Nauki, 03028 Kiev, Ukraine*
[2]*Institute for Problems of Materials Science, National Academy of Science of Ukraine, 3, Krjijanovskogo, 03142 Kiev, Ukraine*
[3]*Center for Nanophase Materials Science, Oak Ridge National Laboratory, Oak Ridge, Tennessee 37831, USA*
[4]*Department of Materials Science and Engineering, Pennsylvania State University, University Park, Pennsylvania 16802, USA*

(Received 25 January 2012; accepted 17 March 2012; published online 4 April 2012)

Theoretical analysis based on the Landau-Ginzburg-Devonshire theory is used to show that the joint action of flexoelectric effect and rotostriction leads to a large spontaneous in-plane polarization ($\sim$1-5 μC/cm^2) and pyroelectric coefficient ($\sim 10^{-3}$ C/m^{2}K) in the vicinity of surfaces of otherwise non-ferroelectric ferroelastics, such as $SrTiO_3$, with static octahedral rotations. The origin of the improper polarization and pyroelectricity is an electric field we name *flexo-roto field* whose strength is proportional to the convolution of the flexoelectric and rotostriction tensors with octahedral tilts and their gradients. Flexo-roto field should exist at surfaces and interfaces in all structures with static octahedral rotations, and thus, it can induce surface polar states and pyroelectricity in a large class of otherwise nonpolar materials. © *2012 American Institute of Physics*. [http://dx.doi.org/10.1063/1.3701152]

Oxide surfaces and interfaces exhibit intriguing properties such as two-dimensional electron gas, superconductivity,[1,2] charged domain walls,[3] magnetism,[4,5] and multiferroicity.[6] Many oxide surfaces possess strong gradients of strain and octahedral rotations. Octahedral rotations (also called the *antiferrodistortions*) are the most common type of phase transitions involving lattice distortions in perovskite oxide systems.[7] Improper ferroelectricity induced by octahedral rotations is inherent in a number of oxides such as $YMnO_3$,[8] $Ca_3Mn_2O_7$,[9] $CaTiO_3$,[10,11] and their interfaces.[12] Hereafter, we call the phenomena related to octahedral rotations as "roto" effects. Our primary interest is a rotostriction effect that induces the strain or stress proportional to the second powers of the octahedral rotations.It has been shown that strain and stress gradients[13–17] can induce polarization near the surfaces and interfaces via the flexoelectric effect.[18–20] Note that all materials are flexoelectrics,[21] and all materials with static rotations (such as oxygen octahedra rotations) possess rotostriction. The joint action of the flexoelectric effect and rotostriction can thus lead to a ferroelectric polarization at an interface across which the octahedral rotation varies. Therefore, *every* antiferrodistortive boundary, twin wall, interface, and surface can, in principle, possesses the roto-flexo effect. Since most functional oxide systems involve natural or artificial interfaces and surfaces, roto-flexo effects are quite general.

Experimental results show that surface influence systematically changes oxygen octahedral rotation behaviour[22,23] (structural transitions in surface layers). Coexistence of antiferrodistortive and ferroelectric distortions was demonstrated with the help of *ab initio* calculations at perovskite surfaces, such as $PbTiO_3$ (001) surface,[24] while it is absent in $PbTiO_3$ bulk. In particular, the reconstruction of the $PbTiO_3$ (001) surface[25] revealed a single layer of antiferrodistortive structure with oxygen cages counter-rotated by 10° about the titanium ions. Antiferrodistortive reconstruction of the out-of-plane component of octahedral rotation was reached[24] at the PbO-terminated (001) surface and then observed with x-ray scattering.[26] *Ab initio* calculations showed that tensile strain enhances the ferroelectric distortion and suppresses the antiferrodistortive rotation in the vicinity of $PbTiO_3$ (001) surface, while the opposite effect is caused by compressive strain.[27]

Recently, we have theoretically predicted that a combination of flexoelectric effect and rotostriction at oxide interfaces can generate large improper ferroelectricity and pyroelectricity at antiferrodistortive boundaries and elastic twins in $SrTiO_3$ below 105 K.[28] In this letter, we report that a polar state and pyroelectricity are induced by flexo-roto fields in the vicinity of ferroelastic $SrTiO_3$ surface even without any elastic domains.

Using Landau-Ginzburg-Devonshire (LGD) approach, we analyze the behaviour on the polar (P_i) and structural (Φ_i) order parameter (OP) components in the presence of ferroelastic surface. Equations of state are

$$2b_i\Phi_i + 4b^u_{ij}\Phi_j^2\Phi_i - v_{ijkl}\frac{\partial^2\Phi_k}{\partial x_j\partial x_l} - 2r_{mjki}u_{mj}\Phi_k - 2\eta^u_{klij}P_kP_l\Phi_j = 0, \quad (1)$$

$$2a_iP_i + 4a^u_{ijkl}P_jP_kP_l - g_{ijkl}\frac{\partial^2 P_k}{\partial x_j\partial x_l} - 2q_{mjki}u_{mj}P_k - f_{mnil}\frac{\partial u_{mn}}{\partial x_l} - 2\eta^u_{ijkl}P_j\Phi_k\Phi_l = E^d_i, \quad (2)$$

$$c_{ijkl}u_{kl} - r_{ijkl}\Phi_k\Phi_l + f_{ijkl}(\partial P_k/\partial x_l) - q_{ijkl}P_kP_l = \sigma_{ij}. \quad (3)$$

Detailed derivation of Eqs. (1)–(3) is presented in the supplementary material,[29] Sec. S.1 (see also Ref. 28). Φ_i is the components ($i = 1 - 3$) of the structural OP, which is the vector corresponding to the spontaneous octahedral rotation angle around one of their fourfold symmetry axes in a structural phase.[30,33] Note, that the rotation angle is proportional to the displacement (in pm) of an appropriate oxygen atom from its cubic position, as defined by Uwe and Sakudo.[31] P_i is polarization vector, $u_{ij}(\mathbf{x})$ is the strain tensor, $\sigma_{ij}(\mathbf{x})$ is the stress tensor ($i,j = 1-3$). Gradients coefficients g_{ijkl} and v_{ijkl} are regarded positive for commensurate ferroics, η^u_{ijkl} is the biquadratic coupling term,[32–34] f_{ijkl} is the forth-rank tensor of flexoelectric coupling, q_{ijkl} is the forth-rank electrostriction tensor, r_{ijkl} is the rotostriction tensor, and c_{ijkl} is elastic stiffness. The flexoelectric effect tensor f_{ijkl} and rotostriction tensor r_{ijkl} have nonzero components in all phases and for any symmetry of the system. Tensors form for cubic $m3m$ symmetry is well-known; in particular, f_{12}, f_{11}, and f_{44} are nonzero.[35,36] Temperature dependence of coefficients a_i and b_i can be fitted with Barrett law, $a_i(T) = \alpha_T T_q^{(E)}\left(\coth(T_q^{(E)}/T) - \coth(T_q^{(E)}/T_0^{(E)})\right)$, $b_i(T) = \beta_T T_q^{(\Phi)}\left(\coth(T_q^{(\Phi)}/T) - \coth(T_q^{(\Phi)}/T_S)\right)$. In the considered dielectric limit depolarization field components E_i^d (if any exist) are determined self-consistently from Maxwell equation $\varepsilon_0\varepsilon_b\partial E_i^d/\partial x_i = -\partial P_i/\partial x_i$ with corresponding boundary conditions; ε_b is the "background" isotropic lattice permittivity.[37] The system is considered without top electrode. External electric field is regarded absent.

Allowing for the surface energy, $F_S = \int_S (a_i^S P_i^2 + b_i^S \Phi_i^2) d^2r$, Eqs. (1)–(3) should be supplemented with the boundary conditions at $x_3 = 0$ for the OP and polarization vectors,

$$\left(2b_i^S\Phi_i - v_{i3kl}\frac{\partial\Phi_k}{\partial x_l}\right)\Big|_{x_3=0} = 0, \quad (4)$$

$$\left(2a_i^S P_i - g_{i3kl}\frac{\partial P_k}{\partial x_l} + \frac{f_{jki3}}{2}u_{jk}\right)\Big|_{x_3=0} = 0. \quad (5)$$

Third kind boundary conditions (4) and (5) reflect the surface energy contribution into the OP and polarization vector components slope near the surface that can be characterized by so-called extrapolation lengths $\sim v_{i3kl}/2b_i^S$ and $g_{i3kl}/2a_i^S$. The additional source of polarization in Eq. (5), $f_{jki3}u_{jk}/2$, is originated from the flexoelectric effect.[19] Surface energy coefficients a_i^S and b_i^S ($i = 1-3$) are regarded positive and weakly temperature dependent. Note that the values of b_i^S could essentially influence near surface behaviour of the structural OP. For instance, the most likely case $b_3^S \ll b_{1,2}^S$ favors the octahedral rotations around the axis normal to the surface (as it was predicted by *ab initio* calculations for $PbTiO_3$ (Refs. 24, 25, and 27)).

Allowing for the flexoelectric effect boundary condition for elastic stress at mechanically free flat surface acquires the form[38]

$$\left(\sigma_{3i} - \frac{f_{j3i3}}{2}\frac{\partial P_j}{\partial x_3} + \frac{f_{j3il}}{2}\frac{\partial P_j}{\partial x_l}\right)\Big|_{x_3=0} = 0. \quad (6)$$

General mathematical derivation of the boundary condition (6) can be found in Ref. 38. Since inhomogeneous polarization could induce the surface bending via the flexoelectric coupling, Eq. (6) differs from the conventional condition $\sigma_{3i}|_{z=0} = 0$. Compatibility relations should be valid everywhere.

Hereafter, we chose tetragonal $SrTiO_3$ ($T < 105$ K, space group I4/mcm) for numerical simulations, since all necessary parameters including gradient coefficients and flexoelectric tensor are known for the material (see Table S.I, supplementary material[29]). Unfortunately, exact values of gradient coefficients and flexoelectric tensor are unknown for other ferroelastics like $CaTiO_3$ or $EuTiO_3$, but the extension of the obtained results will be valid qualitatively for them, making the flexo-roto field induced polar states at surfaces and interfaces a general phenomenon in nature.

Now let us calculate the depth of the induced polarization penetration from the free surface $x_3 \equiv z = 0$. For the case when 4-fold axis is *parallel* to the mono-domain $SrTiO_3$ surface, the *most thermodynamically preferable* situation is two z-dependent components of OP vector, in-plane $\Phi_{||}(z)$ and out-of plane $\Phi_\perp(z)$, and z-dependent in-plane polarization $P_{||}(z)$ that does not cause any depolarization field ($E_{||}^d = 0$, see the sketch of the problem geometry in Fig. 1(a)). Also one may consider out-of-plane polarization $P_\perp(z)$, but without enough concentration of free carriers its value is strongly affected by the depolarization field

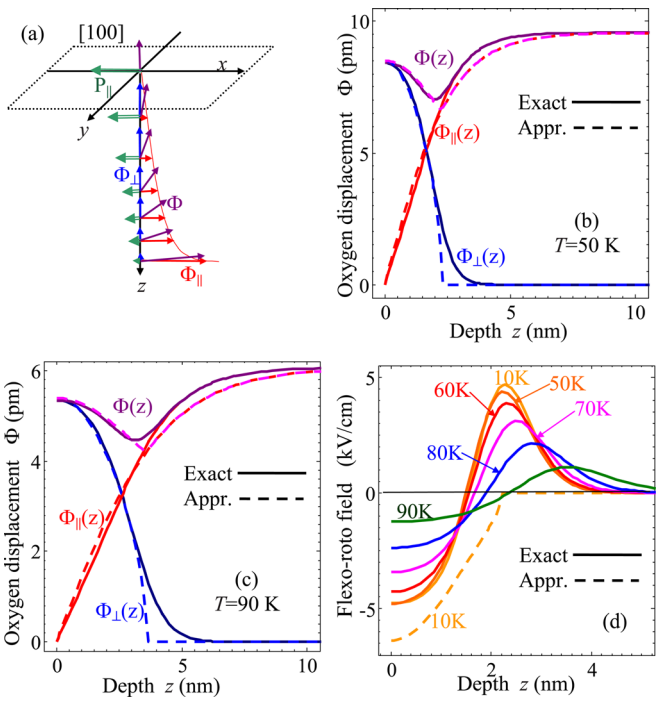

FIG. 1. (a) Sketch of the problem geometry in the vicinity of $SrTiO_3$ [100] cut. 4-fold axis is parallel to the surface. (b) and (c) Depth z-profile of the structural OP components $\Phi_\perp(z)$, $\Phi_{||}(z)$ and absolute value $\Phi(z) = \sqrt{\Phi_\perp^2(z) + \Phi_{||}^2(z)}$ (labels near the curves) calculated numerically from *coupled* equation (3) (solid curves) and analytically from *decoupled* equations (8a) (dashed curves) at temperatures T = 50 K (b) and 90 K (c). $SrTiO_3$ parameters are listed in Table S.I, supplementary material,[29] and the extrapolation length $\lambda_{||} = 0$ is defined after Eq. (8b). (d) Flexo-roto field E_{FR}^B calculated at different temperatures 10, 50, 60, 70, 80, and 90 K (numbers near the curves).

$E_{\perp}^{d} = -P_{\perp}(z)/\varepsilon_0\varepsilon_b$. We calculated numerically that $P_{||}(z)$ values are at least 10^3 times higher than $P_{\perp}(z)$ values without screening by free carriers. For the considered geometry, Eq. (6) reduced to the conventional form $\sigma_{3i}|_{z=0} = 0$ (see supplementary material,[29] Sec. S.3).

For the case when 4-fold axis is *perpendicular* to the mono-domain $SrTiO_3$ surface, the OP becomes normal to the surface (i.e., out-of-plane) in the bulk of the sample. The appearance of in-plane OP components is not likely in this case (see comments after Eq. (2)). As a result, only out-of-plane components of polarization $P_{\perp}(z)$ can be induced. The latter is strongly diminished by the depolarization field. Thus, we do not consider the case here, especially because the length scale of $P_{\perp}(z)$ distribution is of order of lattice constant.

We numerically solve *coupled* systems (1)–(3) when 4-fold axis is *parallel* to the mono-domain $SrTiO_3$ surface. Results are shown in Figs. 1–3. Our numerical simulations performed for coupled equations (1)–(3) with boundary conditions (4)–(6) demonstrate that polarization weakly affects structural OP. The fact makes it possible to *decouple* the polarization vector in systems (1)–(3) that reduces to the form (S.12), supplementary material.[29] The solution for strain and stresses has the form (S.13). Decoupling gives us the possibility to look for approximate analytical expression for OP and polarization. For the considered geometry, decoupled equations for OP components have the form

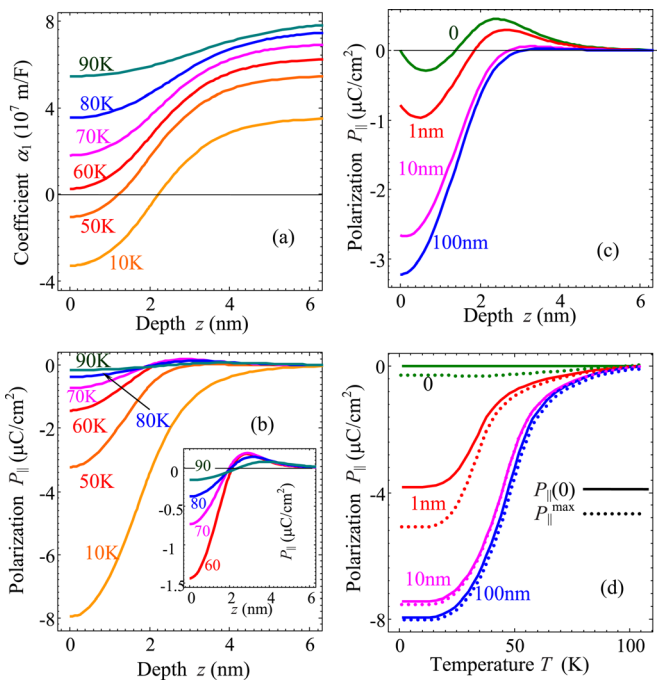

FIG. 2. (a) Coefficient $\alpha_1(z)$ and (b) spontaneous polarization $P_{||}(z)$ vs. the depth z from the surface calculated numerically from coupled equation (3) at different temperatures 10, 50, 60, 70, 80, and 90 K (numbers near the curves) for polarization extrapolation length $\lambda_P = 0$. (c) Polarization $P_{||}(z)$ vs. the depth z calculated for different length $\lambda_P = 0$, 1 nm, 10 nm, 100 nm (figures near the curves) and temperature 50 K. (d) Surface polarization $P_{||}(0)$ (solid curves) and polarization maximal value $P_{||}^{max}(z)$ (dotted curves) vs. temperature calculated for $\lambda_P = 0$, 1 nm, 10 nm, and 100 nm (figures near the curves). Material parameters of $SrTiO_3$ are listed in Table S.I, supplementary material,[29] and structural OP extrapolation length $\lambda_{||} = 0$.

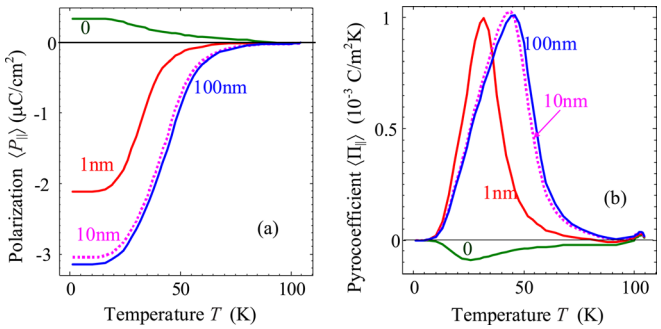

FIG. 3. Temperature dependence of average polarization $\langle P_{||}\rangle$ (a) and pyroelectric coefficient $\langle\Pi_{||}\rangle$ (b) calculated from coupled equation (3) for different length $\lambda_P = 0$, 1 nm, 10 nm, and 100 nm (figures near the curves). Material parameters of $SrTiO_3$ are listed in Table S.I, supplementary material,[29] and [29] the extrapolation length $\lambda_{||} = 0$.

$$2b_{\perp}\Phi_{\perp} + 4b_{11}^{\perp}\Phi_{\perp}^3 + 2b_c\Phi_{\perp}\Phi_{||}^2 - v_{11}\frac{\partial^2\Phi_{\perp}}{\partial z^2} = 0, \qquad (7a)$$

$$2b_{||}\Phi_{||} + 4b_{11}^{||}\Phi_{||}^3 + 2b_c\Phi_{||}\Phi_{\perp}^2 - v_{44}\frac{\partial^2\Phi_{||}}{\partial z^2} = 0, \qquad (7b)$$

where the following designations are introduced: $b_{\perp} = b_1 - \left(b_{12}^u - b_{12}^{\sigma} - \frac{r_{11}r_{12}}{c_{11}} + \frac{r_{44}^2}{2c_{44}}\right)\Phi_B^2$, $b_{11}^{\perp} = b_{11}^u - \frac{r_{11}^2}{2c_{11}}$, $b_{||} = b_1 - 2\left(b_{11}^u - b_{11}^{\sigma} - \frac{r_{12}^2}{2c_{11}}\right)\Phi_B^2$, $b_{11}^{||} = b_{11}^u - \frac{r_{12}^2}{2c_{11}}$, and $b_c = b_{12}^u - \frac{r_{11}r_{12}}{c_{11}} - \frac{r_{44}^2}{2c_{44}}$. Also we used expansion coefficients at given stress, $b_{ijkl}^{\sigma} = b_{ijkl}^u - r_{msji}s_{mspq}r_{pqkl}/2$, here s_{mnij} is the elastic compliances tensor. The bulk value of OP is $\Phi_B(T) = \sqrt{-b_1(T)/2b_{11}^{\sigma}}$. Since the condition $v_{11} \ll v_{44}$ is typically valid due to the fact of strong coupling of octahedron rotations in the layer, perpendicular to rotation axis, and weak coupling between such layers,[39] the second derivative can be neglected in Eq. (7a).[33] So under the condition $b_{\perp} + b_c\Phi_{||}^2(z) < 0$, approximate solution acquires the form

$$\Phi_{\perp}(z) \approx \sqrt{-\frac{1}{2b_{11}^{\perp}}\left(b_{\perp} + b_c\Phi_{||}^2(z)\right)} \qquad (8a)$$

while $\Phi_{\perp}(z) \equiv 0$ and $b_{\perp} + b_c\Phi_{||}^2(z) > 0$. Solution (8a) is not consistent with the boundary condition (4a) for $\Phi_{\perp}(0)$ in general case, but our numerical simulations proved that the influence of the boundary condition becomes negligible even at very small distances from the surface. This happens because corresponding length scale $L_{\perp}(T) = \sqrt{v_{11}/|b_{\perp}(T)|}$ is smaller that the lattice constant making approximation (8a) self-consistent. Solution for the OP component $\Phi_{||}(z)$ was derived by direct variation method as

$$\Phi_{||}(z) \approx \Phi_B \cdot \tanh\left(\frac{z - z_0}{L_{\Phi}}\right) \approx \Phi_B\left(1 - \frac{1}{1 + \sqrt{2}\lambda_{||}/L_{\Phi}}\exp\left(-\frac{\sqrt{2}z}{L_{\Phi}}\right)\right). \qquad (8b)$$

Correlation length is introduced as $L_{\Phi}(T) = \sqrt{2v_{44}/|b_{||}(T)|}$; the extrapolation lengths for "in-plane" component of OP is introduced as $\lambda_{||} = v_{44}/b_1^S$. The length is determined by the

surface energy coefficient $b_1^S \geq 0$. Hereinafter, we regard the extrapolation length to be not negative, otherwise higher positively defined terms should be included in the surface energy $\int_S b_i^S \Phi_i^2 d^2r$. Note, that the case $\lambda_{||} = 0$ (i.e., $z_0 = 0$) corresponds to maximal possible amplitude $\Phi_\perp(0) = \max$ and minimal $\Phi_{||}(0) = 0$ [as shown in Fig. 1(b)]. At arbitrary $\lambda_{||}$ constant z_0 found from the boundary condition (4a) is $z_0 = L_\Phi \times \operatorname{actanh}\left((\lambda_{||}/L_\Phi)(0.5 + \sqrt{0.25 + (\lambda_{||}/L_\Phi)^2})^{-1}\right)$. The gradient region under the surface has the maximal depth exactly for the case of $z_0 = 0$. In the general case, the characteristic depth of the gradient region is about several L_Φ.

Numerical simulations proved that the approximate analytical expressions (8a) relatively accurately reproduce the OP distribution calculated numerically from Eq. (3) and their gradients in the near-surface region (see Figs. 1(b) and 1(c)).

Using the elastic solutions (S.3)–(S.4) and decoupling approximation, we simplify equation for polarization $\partial F_b/\partial P_i = 0$ as

$$\alpha_1(z)P_{||} + \left(4a_{11}^u - 2\frac{q_{12}^2}{c_{11}}\right)P_{||}^3 - \left(g_{44} - \frac{f_{44}^2}{c_{44}}\right)\frac{\partial^2 P_{||}}{\partial z^2} = E_{FR}^B(z), \tag{9a}$$

$$\left(P_{||} - \lambda_P \frac{\partial P_{||}}{\partial z} + P_{FR}^S\right)\Big|_{z=0} = 0. \tag{9b}$$

Polarization extrapolation length is introduced as $\lambda_P = g_{44}/2a_1^S$, whose geometrical sense is described in Ref. 40 The length is determined by the surface energy coefficient a_1^S that depends on the surface state and is poorly known for ferroelectrics.[41] Since λ_P is unknown for $SrTiO_3$, we vary it in the physically realistic range of 1–100 nm.

It follows from Eqs. (9a) that there are several sources of the polarization appearance in the vicinity of surface. The first source is the inhomogeneity in the right-hand-side of Eq. (9a): electric field $E_{FR}^B(z) = (r_{44}f_{44}/c_{44})\partial(\Phi_{||}\Phi_\perp)/\partial z$, which strength is proportional to the convolution of the flexoelectric and rotostriction tensors with OP gradient, further regarded as *gradient flexo-roto field*. The depth profile of $E_{FR}(z)$ is shown in Fig. 1(d). The second source is the inhomogeneity in the boundary condition (9b), $P_{FR}^S = \left(r_{44}f_{44}/(4c_{44}a_1^S)\right)\Phi_{||}(0)\Phi_\perp(0)$, whose strength is also proportional to the convolution of the flexoelectric and rotostriction tensors with OP, further regarded as *built-in surface flexo-roto polarization*. Both these sources induce *improper spontaneous polarization*. Note, that $P_{FR}^S = 0$ for the case $\lambda_{||} = 0$, since $\Phi_{||}(0) = 0$.

The condition $\alpha_1(z) < 0$, which is valid near the surface at low temperatures, can lead to the *roto-induced ferroelectric polarization* appearance under negligibly small depolarization field. Estimations made for $SrTiO_3$ parameters prove that coefficient

$$\alpha_1(z) = 2\left(a_1 - \left(\eta_{11}^u + \frac{q_{12}r_{12}}{c_{11}}\right)\Phi_{||}^2(z) - \left(\eta_{11}^\sigma - \eta_{11}^u - \frac{q_{12}r_{12}}{c_{11}}\right)\Phi_B^2 - \left(\eta_{12}^u + \frac{q_{12}r_{11}}{c_{11}}\right)\Phi_\perp^2(z)\right) \tag{10}$$

is positive in the single-domain bulk material at temperature $T < T_S$, where $\Phi_{||}(z) \approx \Phi_B$ (otherwise, a bulk material should be ferroelectric). Here, we re-introduced the biquadratic coupling coefficient $\eta_{ijkl}^\sigma = \eta_{ijkl}^u + q_{msji}s_{mspq}r_{pqkl}$. However, $\alpha_1(z)$ is strongly coordinate-dependent near the surface $z = 0$ as shown in Fig. 2(a). For $SrTiO_3$ parameters, $\alpha_1 > 0$ at temperatures $T > 50$ K and it becomes negative due to the biquadratic coupling at $T < 50$ K.

Nonlinearity and gradients terms can be omitted in Eq. (9a) in the region where $\alpha_1 > 0$, leading to the simple approximate expression for polarization and pyroelectric coefficient distribution,

$$P_{||}(z) \sim \frac{f_{44}r_{44}}{\alpha_1(z)c_{44}}\frac{\partial(\Phi_{||}\Phi_\perp)}{\partial z}, \tag{11a}$$

$$\Pi_{||}(z) = \frac{dP_{||}(z)}{dT} \sim \frac{f_{44}r_{44}}{c_{44}}\frac{d}{dT}\left(\frac{\partial(\Phi_{||}\Phi_\perp)}{\alpha_1(z)\partial z}\right). \tag{11b}$$

Spontaneous polarization (11a) is "incipient" as induced by the flexo-roto coupling, and thus, no ferroelectric hysteresis exists at temperatures $T > 50$ K. True ferroelectricity appears and hysteresis loop opens for $\alpha_1 < 0$, that is possible at $0 \leq z \leq 6$ nm and $T > 50$ K.

From Fig. 2(b), we can conclude that the flexo-roto fields do induce polar state under the surface at distances $z \leq 2L_\Phi$ in ferroelastics. Note, that $L_\Phi \sim 3$ nm for $SrTiO_3$ at $T < 90$ K (Ref. 28 and 33) determines the nanometer scale of the surface polar state. So, the typical thickness of polar state is about 7 lattice constants, making continuum theory results at least semi-quantitatively valid. Polarization appears at temperatures lower than T_S and it increases as the temperature decreases (compare different curves in Fig. 2(b)). Surface polarization and maximal values increase as the extrapolation length λ_P increases (compare different curves in Fig. 2(d)). For small λ_P, polarization may change its sign in the interface region (see Fig. 2(c)). It is seen that spontaneous polarization can reach noticeable values $\sim$1–10 $\mu C/cm^2$ in the gradient region $z \leq 2L_\Phi$ at temperatures lower than 60 K.

Temperature dependence of polarization $\langle P_{||} \rangle$ averaged over the polar layer thickness $w = 5$ nm is shown in Fig. 3(a). Temperature dependence of pyroelectric coefficient $\langle \Pi_{||} \rangle$ averaged over the polar layer thickness $w = 5$ nm is shown in Fig. 3(b). We calculated noticeable pyroelectric coefficient $\langle \Pi_{||} \rangle \sim 2 \times 10^{-3}$ C/m^{2}K. The values are well above detectable limits of pyroelectric coefficient, which are about 10^{-6} C/m^{2}K.[42] Thus, either planar electrode setup or PyroSPM (Ref. 43) supplied with sharp tips of sizes 5-10 nm could reliably detect local lateral pyroelectric response of the ferroelastic surface.

To summarize, we report a new source of field, we name the gradient *flexo-roto field*, which induces a significant improper spontaneous polarization and pyroelectricity in the vicinity of surfaces and interfaces of otherwise non-ferroelectric ferroelastics such as $SrTiO_3$, and by extension in $CaTiO_3$, $EuTiO_3$, and in antiferroelectrics like $PbZrO_3$. In $SrTiO_3$ flexo-roto effect leads to a large spontaneous polarization ($\sim$1–5 $\mu C/cm^2$) and pyroelectric coefficient ($\sim 10^{-3}$ C/m^{2}K). The strength of the gradient flexo-roto field is proportional to the convolution of the flexoelectric and

rotostriction tensors with the gradients of octahedral rotations, which are structural order parameters. The strength of the surface flexo-roto polarization is proportional to the convolution of the flexoelectric and rotostriction tensors with octahedral rotations on the surface. Flexo-roto effects should exist at surfaces in all structures with static rotations, which are abundant in nature, it allows for contribution into polar interfaces in a large class of nonpolar materials.

Note, that there are other possible reasons for polar surface states in nonpolar materials such as $SrTiO_3$: space charge due to defect chemistry and band gap differences between surfaces and bulk,[44] surface reconstruction and atom clustering,[45] surface piezoelectricity,[46,47] and strained polar regions that extends into the bulk at a distance much larger than a few nanometers.[48] In accordance with these and other studies, combined rotostriction and flexoelectricity cannot not be the sole contribution to the polar surface stats in ferroelastics. However, the conclusion in this letter is that the surfaces of all ferroelastics with octahedral tilts should be intrinsically polar in the low temperature octahedrally tilted phase.

Authors gratefully acknowledge multiple discussions with S.L. Bravina (NASU) and Zheng Gai (ORNL). A.N.M. and G.S.S. acknowledges the National Academy of Sciences of Ukraine for support. Research supported (SVK) by the U.S. Department of Energy, Basic Energy Sciences, Materials Sciences and Engineering Division. V.G. and L.Q.C. would like to acknowledge funding from the National Science Foundation Grant Nos. DMR-0908718 and DMR-0820404.

[1]A. Ohtomo, D. A. Muller, J. L. Grazul, and H. Y. Hwang. Nature **419**, 378 (2002).
[2]J. W. Park, D. F. Bogorin, C. Cen, D. A. Felker, Y. Zhang, C. T. Nelson, C. W. Bark, C. M. Folkman, X. Q. Pan, M. S. Rzchowski, J. Levy, and C. B. Eom, Nat. Commun. **1**, 94 (2010).
[3]J. Seidel, L. W. Martin, Q. He, Q. Zhan, Y.-H. Chu, A. Rother, M. E. Hawkridge, P. Maksymovych, P. Yu, M. Gajek, N. Balke, S. V. Kalinin, S. Gemming, F. Wang, G. Catalan, J. F. Scott, N. A. Spaldin, J. Orenstein, and R. Ramesh, Nature Mater. **8**, 229 (2009).
[4]Y.-H. Chu, L. W. Martin, M. B. Holcomb, M. Gajek, S.-J. Han, Q. He, N. Balke, C.-H. Yang, D. Lee, W. Hu, Q. Zhan, P.-L. Yang, A. Fraile-Rodríguez, A. Scholl, S. X. Wang, and R. Ramesh, Nature Mater. **7**, 478 (2008).
[5]S. J. May, P. J. Ryan, J. L. Robertson, J.-W. Kim, T. S. Santos, E. Karapetrova, J. L. Zarestky, X. Zhai, S. G. E. te Velthuis, J. N. Eckstein, S. D. Bader, and A. Bhattacharya, Nature Mater. **8**, 892 (2009).
[6]M. Stengel, D. Vanderbilt, and N. A. Spaldin, Nature Mater. **8**, 392 (2009).
[7]V. Gopalan and D. B. Litvin, "Rotation-reversal symmetries in crystals and handed structures," Nature Mater. **10**, 376–381 (2011).
[8]C. J. Fennie and K. M. Rabe, Phys. Rev. B **72**, 100103(R) (2005).
[9]N. A. Benedek and C. J. Fennie, Phys. Rev. Lett. **106**, 107204 (2011).
[10]L. Goncalves-Ferreira, S. A. T. Redfern, E. Artacho, and E. K. H. Salje, Phys. Rev. Lett. **101**, 097602 (2008).
[11]S. Van Aert, S. Turner, R. Delville, D. Schryvers, G. Van Tendeloo, and E. K. H. Salje, Adv. Mater. **24**, 523–527 (2012).
[12]E. Bousquet, M. Dawber, N. Stucki, C. Lichtensteiger, P. Hermet, S. Gariglio, J.-M. Triscone, and P. Ghosez, Nature **452**, 732 (2008).
[13]D. A. Tenne, A. Bruchhausen, N. D. Lanzillotti-Kimura, A. Fainstein, R. S. Katiyar, A. Cantarero, A. Soukiassian, V. Vaithyanathan, J. H. Haeni, W. Tian, D. G. Schlom, K. J. Choi, D. M. Kim, C. B. Eom, H. P. Sun, X. Q. Pan, Y. L. Li, L. Q. Chen, Q. X. Jia, S. M. Nakhmanson, K. M. Rabe, and X. X. Xi, Science **313**, 1614 (2006).
[14]A. Vasudevarao, A. Kumar, L. Tian, J. H. Haeni, Y. L. Li, C.-J. Eklund, Q. X. Jia, R. Uecker, P. Reiche, K. M. Rabe, L. Q. Chen, D. G. Schlom, and V. Gopalan, Phys. Rev. Lett. **97**, 257602 (2006).
[15]E. V. Bursian and O. I. Zaikovskii, Fiz. Tverd. Tela **10**, 1413 (1968) [Sov. Phys. Solid State **10**, 1121 (1968)]; E. V. Bursian, O. I. Zaikovsky, and K. V. Makarov, J. Phys. Soc. Jpn **28**, 416 (1970).
[16]W. Ma and L. E. Cross, Appl. Phys. Lett. **79**, 4420 (2001).
[17]W. Ma and L. E. Cross, Appl. Phys. Lett. **88**, 232902 (2006).
[18]E. A. Eliseev, A. N. Morozovska, M. D. Glinchuk, B. Y. Zaulychny, V. V. Skorokhod, and R. Blinc, Phys. Rev. B. **82**, 085408 (2010).
[19]E. A. Eliseev, A. N. Morozovska, M. D. Glinchuk, and R. Blinc, Phys. Rev. B. **79**, 165433 (2009).
[20]M. S. Majdoub, P. Sharma, and T. Cagin, Phys. Rev. B **77**, 125424 (2008).
[21]A. K. Tagantsev, Phys. Rev. B **34**, 5883 (1986).
[22]R. G. Moore, J. Zhang, V. B. Nascimento, R. Jin, J. Guo, G. T. Wang, Z. Fang, D. Mandrus, and E. W. Plummer, Science **318**, 615 (2007).
[23]R. G. Moore, V. B. Nascimento, J. Zhang, J. Rundgren, R. Jin, D. Mandrus, and E. W. Plummer, Phys. Rev. Lett. **100**, 066102 (2008).
[24]C. Bungaro and K. M. Rabe, Phys. Rev. B **74**, 174111 (2006).
[25]A. Munkholm, S. K. Streiffer, M. V. Ramana Murty, J. A. Eastman, C. Thompson, O. Auciello, L. Thompson, J. F. Moore, and G. B. Stephenson, Phys. Rev. Lett. **88**, 016101 (2002).
[26]M. Sepliarsky, M. G. Stachiotti, and R. L. Migoni, Phys. Rev. B **72**, 014110 (2005).
[27]Y. Umeno, T. Shimada, T. Kitamura, and C. Elsässer, Phys. Rev. B **74**, 174111 (2006).
[28]A. N. Morozovska, E. A. Eliseev, M. D. Glinchuk, L.-Q. Chen, and V. Gopalan, Phys. Rev. B **85**, 094107 (2012).
[29]See supplementary material at http://dx.doi.org/10.1063/1.3701152 for details about the form and structure of free energy, equations of state, and boundary conditions.
[30]N. A. Pertsev, A. K. Tagantsev, and N. Setter, Phys. Rev. B **61**, R825 (2000).
[31]H. Uwe and T. Sakudo, Phys. Rev. B **13**, 271 (1976).
[32]M. J. Haun, E. Furman, T. R. Halemane, and L. E. Cross, Ferroelectrics **99**, 55 (1989); **99**, 13 (1989).
[33]A. K. Tagantsev, E. Courtens, and L. Arzel, Phys. Rev. B **64**, 224107 (2001).
[34]B. Houchmanzadeh, J. Lajzerowicz, and E. Salje, J. Phys.: Condens. Matter **3**, 5163 (1991).
[35]P. Zubko, G. Catalan, A. Buckley, P. R. L. Welche, and J. F. Scott, Phys. Rev. Lett. **99**, 167601 (2007).
[36]J. Hong and D. Vanderbilt, Phys. Rev. B **84**, 180101(R) (2011).
[37]A. K. Tagantsev and G. Gerra, J. Appl. Phys. **100**, 051607 (2006).
[38]A. S. Yurkov, JETP Lett. **94**(6), 455 (2011).
[39]W. Cao and R. Barsch, Phys. Rev. B **41**, 4334 (1990).
[40]R. Kretschmer and K. Binder, Phys. Rev. B **20**, 1065 (1979).
[41]C.-L. Jia, V. Nagarajan, J.-Q. He, L. Houben, T. Zhao, R. Ramesh, K. Urban, and R. Waser, Nature Mater. **6**, 64 (2007).
[42]S. B. Lang, Phys. Today **58**(8), 31 (2005).
[43]J. Groten, M. Zirkl, G. Jakopic, A. Leitner, and B. Stadlober, Phys. Rev. B **82**, 054112 (2010).
[44]E. Heifets, R. I. Eglitis, E. A. Kotomin, J. Maier, and G. Borstel, Surf. Sci. **513**, 211 (2002).
[45]R. Herger, P. R. Willmott, O. Bunk, C. M. Schleputz, B. D. Patterson, and B. Delley, Phys. Rev. Lett. **98**, 076102 (2007).
[46]A. Kholkin, I. Bdikin, T. Ostapchuk, and J. Petzelt, Appl. Phys. Lett. **93**, 222905 (2008).
[47]S. Dai, M. Gharbi, P. Sharma, and H. S. Park, J. Appl. Phys. **110**, 104305 (2011).
[48]H. W. Jang, A. Kumar, S. Denev, M. D. Biegalski, P. Maksymovych, C. W. Bark, C. T. Nelson, C. M. Folkman, S. H. Baek, N. Balke, C. M. Brooks, D. A. Tenne, D. G. Schlom, L. Q. Chen, X. Q. Pan, S. V. Kalinin, V. Gopalan, and C. B. Eom, Phys. Rev. Lett. **104**, 197601 (2010).